BULLETIN OF THE POLISH ACADEMY OF SCIENCES
TECHNICAL SCIENCES, Vol. 69(5), 2021, Article number: e137549
DOI: 10.24425/bpasts.2021.137549

Investigations of TiO_2, Ti/TiO_2 and $Ti/TiO_2/Ti/TiO_2$ coatings produced by ALD and PVD methods on Mg-(Li)-Al-RE alloy substrates

Marcin STASZUK[1*], Łukasz REIMANN[1], Aleksandra ŚCIŚLAK[1], Justyna JAWORSKA[1], Mirosława PAWLYTA[1], Tomasz MIKUSZEWSKI[2], Dariusz KUC[2], Tomasz TAŃSKI[1], and Antonín KŘÍŽ[3]

[1] Silesian University of Technology, Faculty of Mechanical Engineering, ul. Konarskiego 18a, 44-100 Gliwice, Poland
[2] Silesian University of Technology, Faculty of Materials Engineering and Metallurgy, ul. Krasińskiego 8, Katowice, Poland
[3] University of West Bohemia, Faculty of Mechanical Engineering, Univerzitni 22 St., 30614 Plzen, Czech Republic

Abstract. Magnesium alloys have recently become increasingly popular in many sectors of the industry due to their unique properties, such as low density, high specific strength, vibration damping ability along with their recyclability and excellent machinability. Nowadays, thin films have been attracting more attention in applications that improve mechanical and corrosion properties. The following alloys were used for the coated Mg-Al-RE and the ultra-light magnesium-lithium alloy of the Mg-Li-Al-RE type. A single layer of TiO_2 was deposited using the atomic layer deposition ALD method. Multiple layers of the Ti/TiO_2 and $Ti/TiO_2/Ti/TiO_2$ type were obtained by the MS-PVD magnetron sputtering technique. Samples were investigated by scanning and a transmission electron microscope (SEM, TEM) and their morphology was studied by an atomic forces microscope (AFM). Further examinations, including electrochemical corrosion, roughness and tribology, were also carried out. As a result of the research, it was found that the best electrochemical properties are exhibited by single TiO_2 layers obtained by the ALD method. Moreover, it was found that the $Ti/TiO_2/Ti/TiO_2$ double film has better properties than the Ti/TiO_2 film.

Key words: ALD; PVD; TiO_2; magnesium alloys; corrosion resistant.

1. INTRODUCTION

Over the last few decades, there has been an increase in interest in magnesium and its alloys due to their unique properties. The advantages of magnesium include low density $\left(1.74\ g/cm^3\right)$, high strength and specific stiffness, vibration damping ability and good machinability. It is used in many industrial sectors, but primarily in the automotive, aviation, 3C electronics, biomedical and energy industries. Despite many advantages, magnesium and its alloys also have disadvantages, which include: low hardness and poor corrosion resistance [1]. Such drawbacks effectively prevent the use of magnesium and its alloys as the main construction materials produced on a large scale [2]. Magnesium-lithium alloys are classified as ultra-light alloys with a very light structure. They are characterized by low density, strength and stiffness properties, good damping properties and final deformation. Mg-Li alloys are widely used in many industries such as electronics, military, aerospace and the automotive one [3–7]. The mechanical properties of magnesium alloys can be effectively improved by modifying the chemical composition as well as heat and plastic treatment. To improve wear resistance and corrosion resistance, many surface modification techniques are used without changing the base material properties, including vapor deposition processes [1, 8, 9]. The ALD method allows for deposition of extremely conformal and high-quality barrier layers with controllable thickness, even on complex three-dimensional surfaces [10]. However, a lot of experimental research is still being carried out to create a coating that will effectively protect the magnesium surface against corrosion. A modern method of preventing corrosion of magnesium alloys is coating them with hydrophobic and self-repair coatings [11]. There is a lot of research on the production of thin films, especially of metal oxides, which are characterized by a wide range of physicochemical properties. Such coatings are of great interest due to their potential applications. One of the most promising materials is titanium dioxide [12]. TiO_2 coatings are characterized by high chemical stability, low cost, non-toxicity, good optical and electrical properties, very good hydrophilic and hydrophobic properties, and good photocatalytic properties following exposure to UV light. Due to their antibacterial, anti-fogging, self-cleaning properties, perfectly suited for biomedical materials, they are widely used in various industrial sectors [13]. An important and often used feature of TiO_2 is its high refractive index, which varies from 3.8 for rutile to 2.5–3.0 for anatase. Thanks to all its properties, TiO_2 nanostructures can be used in various industries as self-clean-

*e-mail: marcin.staszuk@polsl.pl

Manuscript submitted 2021-03-08, revised 2021-03-08, initially accepted for publication 2021-04-08, published in October 2021

ing layers or corrosion inhibitors, solar cells, pollution-removing membranes as well as optical and optoelectronic components [14]. In recent decades, nanoparticles such as TiO_2, ZrO_2, and SiC have been used to improve the mechanical and barrier properties, leading to the protection of the substrate against corrosion [15, 16]. The TiO_2 thin film obtained by the magnetron sputtering method is characterized by a homogeneous morphology. The layer is flat, the grains show an aspherical shape of different dimensions, and the grain boundaries are noticeable. Depending on the atomizing power, the coating has different grain sizes. The sputtered film with lower power is characterized by smaller grains, but with sharper shapes [17, 18]. Titanium oxide is distinguished by a wide passive place, reaching the value of volts. It is possible to ensure that good quality protection of formation, abrasion resistance and protection of steel against corrosion processes are provided [19, 20]. Along with the increase of the deposition time of the TiO_2 film, the formation of a parallel structure characteristic of the formation of layers is observed. Increasing the thickness of the layer reduces the amorphous inclusions in the structure. The increase in coating thickness leads to waviness and roughness. Changes in the surface morphology structure have a significant impact on the strength properties and hardness of the layers. The hardness of the film increases with increasing thickness and remains high throughout its depth [21]. TiO_2 coatings show an excellent ability to reduce friction and increase wear resistance. The TiO_2 layer wear is characteristic of plastic deformation with low abrasive and fatigue wear. The use of TiO_2 as a component of the Al_2O_3 hybrid coating, along with an increase in the proportion, causes tribological wear characterized by the effect of particle detachment [22, 23]. The work aimed to investigate the structure as well as electrochemical and tribological properties of Ti/TiO_2 and the $Ti/TiO_2/Ti/TiO_2$ thin films obtained by the magnetron sputtering method and TiO_2 coatings deposited by the ALD method deposited on magnesium alloys AE42 and LAE442.

2. MATERIALS AND METHODS

2.1. Materials

The research used magnesium alloys AE42 (Mg-4Al-2RE) and LAE442 (Mg-4Li-4Al-2RE). Samples made of the alloys with a diameter of 14 mm and a height ranging from 4 to 6 mm were mechanically polished on papers and discs with decreasing gradation. All samples were cleaned in an ultrasonic cleaner successively in acetone and isopropanol and dried with compressed air. After placing the substrates in the working chamber of the sputtering machine and obtaining the appropriate working pressure, ion cleaning was carried out just before sputtering the film on. Two types of coatings were made using the PVD method: Ti/TiO_2 and $Ti/TiO_2/Ti/TiO_2$, using the Kurt J. Lesker PVD 75 sputtering machine. In the PVD process, to obtain the tested coatings, a pure titanium target as well as argon Ar (99.9999%) and oxygen O_2 (99.9999%) process gases were used. The coatings were obtained in the DC mode, the magnetron power was 200 W, and process temperature stood at 100°C. The deposition times of individual layers were respectively 2/120 (minutes) for the Ti/TiO_2 coating and 2/60/2/60 (minutes) for the $Ti/TiO_2/Ti/TiO_2$ coating. The deposition speed of layers by the PVD method was Ti = 15 nm/min, TiO_2 = 46 nm/h, and the thickness of the layers was: Ti/TiO_2 = 122nm and $Ti/TiO_2/Ti/TiO_2$ = 152 nm.

A Beneq P400 ALD reactor was used for the thermal ALD deposition of TiO_2. Films were grown on Mg-(Li)-Al-RE substrates without any pre-treatment at a deposition temperature of 70°C. Silicon wafer pieces were used as monitor samples for thickness and RI measurements by means of ellipsometry. The precursors used were $TiCl_4$ and H_2O, and the total ALD cycle was 1,545 cycles. The number of cycles was selected to obtain a thickness of the deposited layers of 100 nm.

2.2. Structure

The topography was examined with the atomic force microscope AFM (XE-100 Park Systems scanning probe microscope). Measurements were made in a non-contact mode in the areas of 1×1 μm, 10×10 μm and 20×20 μm.

Scanning electron microscope SEM (Supra35-Carl Zeiss AG) was used to examine the structure of investigated materials and damage resulting from abrasion and corrosion resistance tests. Energy dispersive X-ray spectroscopy EDS for was used for chemical analysis of samples in micro areas. The tests were performed with an accelerating voltage of 10 kV.

The investigations of the thin foil structure were performed with the use of the FEI Titan 80–300 high-resolution transmission electron microscope (HRTEM). The analyzes of the chemical composition in micro areas were performed with the use of EDS and EELS spectroscopic methods. The tests were performed at an accelerating voltage of 300 kV.

The surface roughness of the samples was tested on a Mitutoyo SJ-210 contact profilometer. Measurements were made on each sample, along a 4.8 mm section. Based on the obtained roughness measurement results, the arithmetic means, standard deviation and confidence interval were calculated for each sample.

2.3. Corrosion and wear resistance test

The potentiodynamic method and the EIS method were used to determine the corrosion resistance of the samples using the potentiostat-galvanostat ATLAS 0531 EU&IA. DC tests were carried out in the vessel, a three-electrode system was used, in an environment of 0.05M NaCl solution under the risk of local (pitting) corrosion. A saturated silver-plated electrode was used as a reference electrode, while a platinum plate was used as an auxiliary electrode.

The wear resistance tests were performed on a CSM Instruments tribometer in the ball-on-disc mode in an air atmosphere at room temperature. 6 mm diameter Al_2O_3 aluminum oxide balls were used as counter-samples. The tests were performed with the use of the following parameters: wear diameter 5 mm, linear speed v = 0.5 cm/s, normal force F_n = 0.5 N. During the test, the friction coefficient was recorded as a function of the number of cycles. The tests were performed for the maximum number of cycles of 500 (one cycle is equal to one full revolution of the sample).

(a)

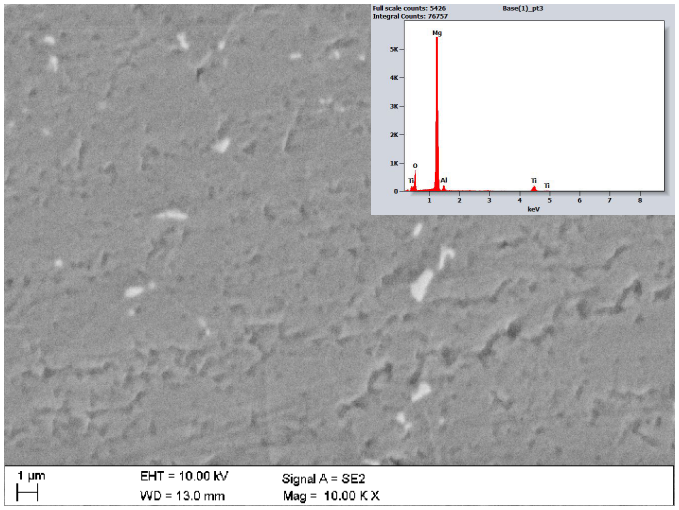

(b)

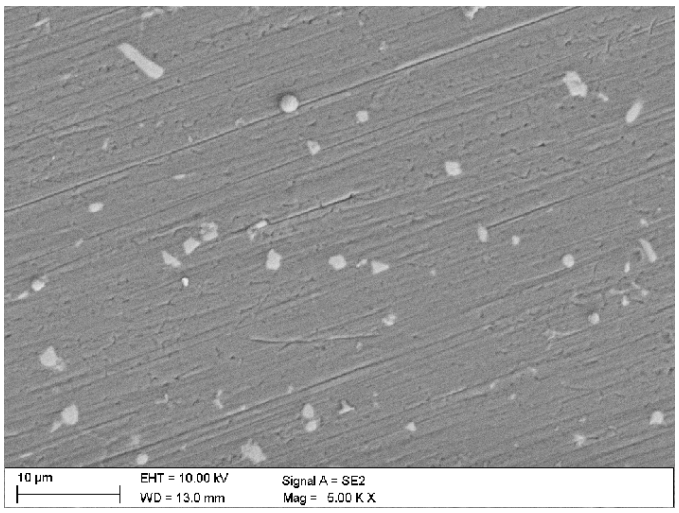

(c)

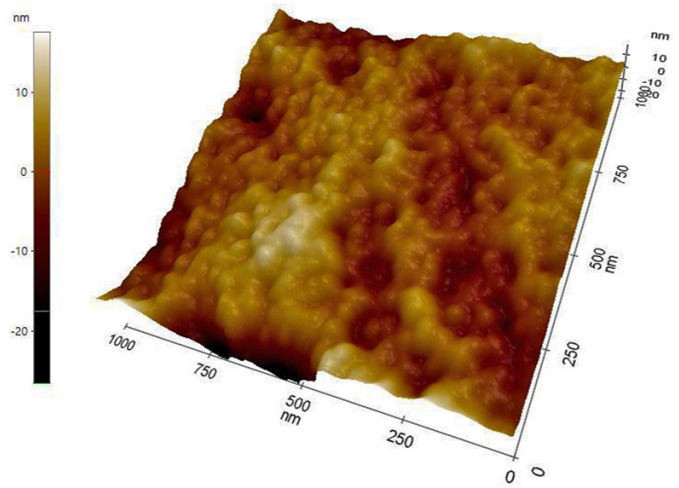

Fig. 1. Morphology of the sample based on AE42 alloy with a) Ti/TiO_2 coatings (SEM + EDS), b) Ti/TiO_2/Ti/TiO_2 coatings (SEM), c) Ti/TiO_2/Ti/TiO_2 coatings (AFM)

3. RESULTS

3.1. Surface morphology

Figure 1 shows the initial state of the morphology of PVD coatings obtained as a result of the deposition. They are characterized by a relatively uniform structure. The coatings do not show sharp shapes. Moreover, oxide agglomerates appear on the surfaces, which are more numerous in the case of the LAE442 alloy sample. As a result of EDS tests, there are peaks of magnesium and aluminum from the base material. Visible reflections of titanium confirm its presence on the sample surface (Fig. 1a). As a result of the surface roughness measurements, it was found that the roughness parameter Ra is in the range from 0.036 µm to 0.126 µm (Fig. 2). The increase in surface roughness in the case of ALD coatings as compared to the uncoated substrate is slight. A clear increase in surface roughness is shown by PVD-coated surfaces in comparison with the uncoated surface, for which the average roughness difference is 0.07 µm. It should also be emphasized that in each case the surface roughness of magnesium-lithium alloys shows higher Ra values than the surfaces of lithium-free alloys. In the images from the AFM microscope, more distinct roughness of the coating with sharper shapes was observed in the case of the coated sample.

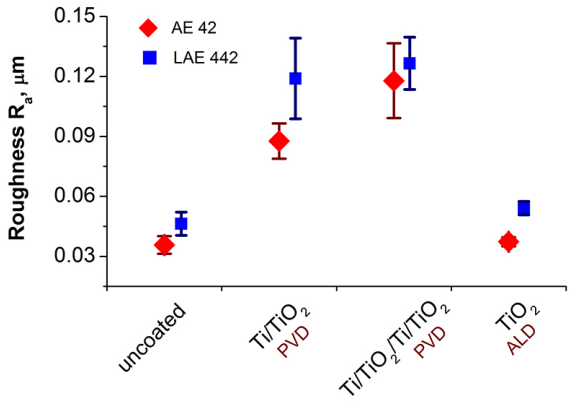

Fig. 2. Roughness R_a values of investigated samples

3.2. Corrosion test

In all tested cases, there is the hysteresis loop which proves the initiation and development of pitting corrosion processes (Fig. 3). In the case of polarization curves for samples with a titanium oxide layer, a narrower hysteresis loop was observed, which proves that it is less susceptible to pitting as compared with uncoated samples. Wider loops are also present in samples of the LAE442 alloy, which indicates a higher corrosion potential (Fig. 3). Coatings with a double layer of titanium oxide show the lowest corrosion potential, indicating that they are not very resistant to corrosion. Samples with ALD, both for AE42 and LAE442 alloys, show the lowest corrosion current density and the highest polarization resistance values (Table 1).

Electrochemical impedance spectroscopy research, showed in Fig. 4 in the form of Nyquist impedance diagrams and in Fig. 5 as Bode plots, presents the relationship of log|Z| and phase angle max versus log frequency. Higher log|Z| and

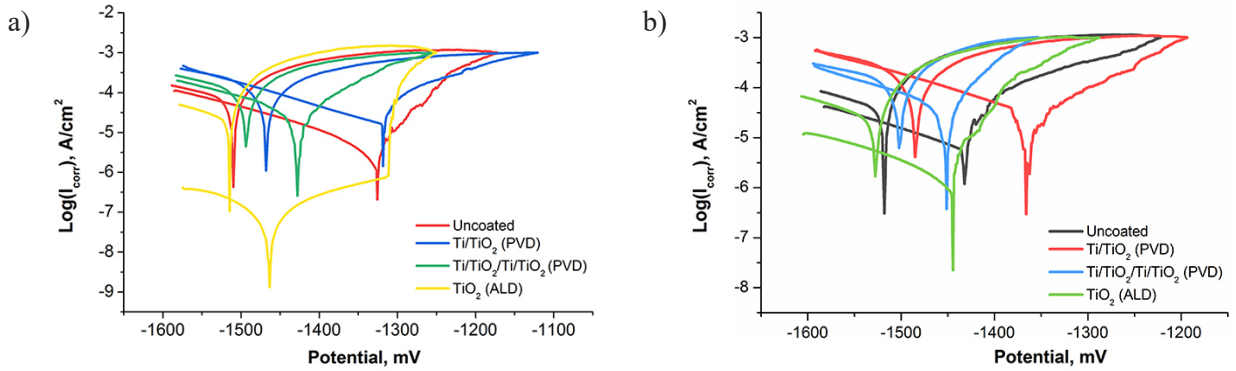

Fig. 3. Potentiodynamic polarization curves for a) AE42, b) LAE442

Table 1

Potentiodynamic polarization parameters for samples in 0.05 m NaCl solution

Substrate	Coating	E_{corr} [mV]	I_{corr} [μA/cm²]	R_{pol} [Ohm×cm²]	Substrate	Coating	E_{corr} [mV]	I_{corr} [μA/cm²]	R_{pol} [Ohm×cm²]
AE 42	Uncoated	–1328	3.80	4250	LAE442	Uncoated	–1430	5.49	1049
	Ti/TiO_2	–1320	16	716.3		Ti/TiO_2	–1380	5.2	977.9
	$Ti/TiO_2/Ti/TiO_2$	–1426	10.98	976.78		$Ti/TiO_2/Ti/TiO_2$	–1452	11.21	522.63
	TiO_2	–1466	0.07	329×10^3		TiO_2	–1447	0.85	5729

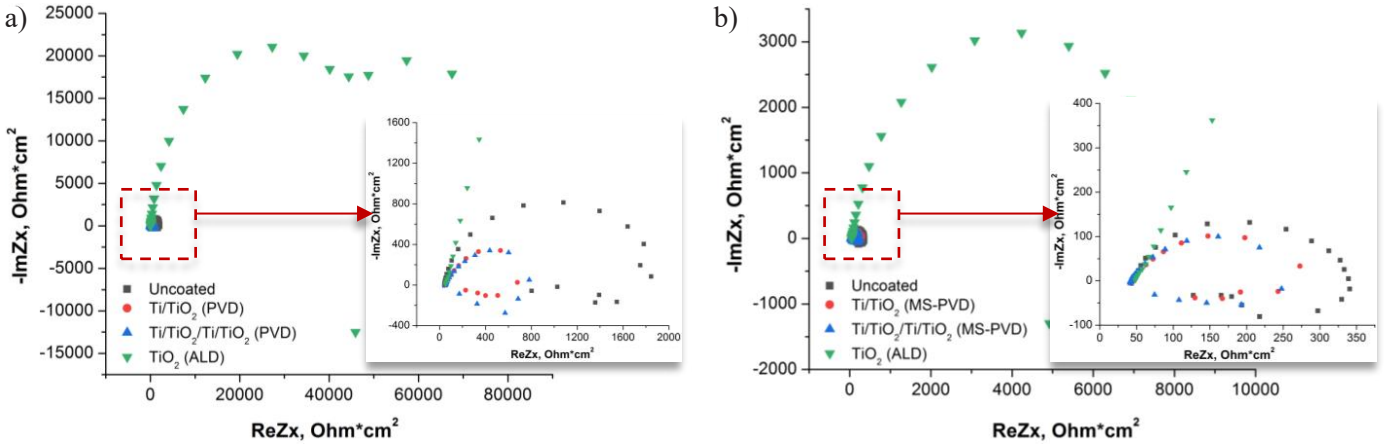

Fig. 4. Nyquist impedance diagram for a) AE42, b) LAE442

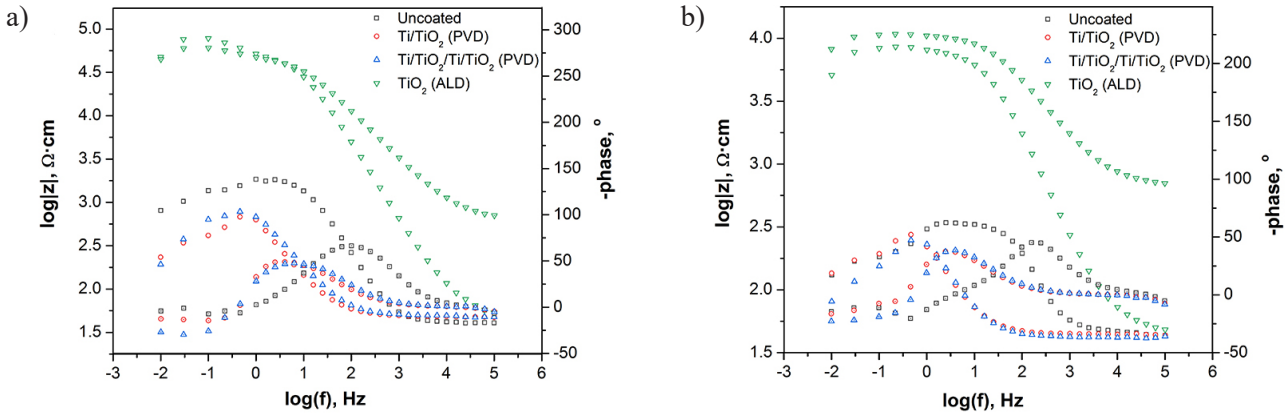

Fig. 5. Bode impedance diagram for a) AE42, b) LAE442

Table 2
Electrochemical impedance spectroscopy parameters

Substrate	Coating	R1 [Ohm]	Q2 $[\mu F \times s^{(\alpha-1)}]$	a2	R2 [Ohm]	L1 $[H \times cm^{-2}]$	R3 [Ohm]
AE 42	Uncoated	41.11	9.5	0.93	1722	355.6	1932
	Ti/TiO_2	48.33	297.2	0.80	806.2	599.4	320
	$Ti/TiO_2/Ti/TiO_2$	49.04	205	0.81	792.4	1756	154.7
	TiO_2	49.64	475.8	0.85	7476	2.307	9.62
LAE 442	Uncoated	45.44	13.42	0.92	293.8	141.9	165.2
	Ti/TiO_2	46.11	475	0.97	220.7	511.2	120.5
	$Ti/TiO_2/Ti/TiO_2$	42.32	547	0.88	204.1	307.4	48.81
	TiO_2	44.52	2.93	1	24,650	2.93	72,430

higher θ_{max} represent better corrosion resistance. The impedance spectra for all samples have a distinct semicircle, indicating that the electrode response is controlled by the charge transfer rate. Moreover, the spectra exhibit a characteristic "wrap" at the end of the low-frequency range, which indicates that some inductive properties of the spectrum are revealed. The highest values of ImZ and ReZ were recorded for the samples coated with the ALD method. ImZ values are, respectively, 22,000 $\Omega \times cm^2$ for the sample based on the AE42 alloy and 3000 $\Omega \times cm^2$ for LAE442.

These values are distinctly higher than those of the uncovered samples, which are 800 $\Omega \times cm^2$ for the AE42 alloy and 140 $\Omega \times cm^2$ for LAE442. In the case of PVD-coated samples, the values are 400 $\Omega \times cm^2$ for AE42 alloy and 100 $\Omega \times cm^2$ for LAE442. The graphs show that the samples based on the AE42 alloy had higher corrosion resistance. Bode plots show an analogous relationship. The uncoated sample of the AE42 alloy exhibited a phase shift angle of 68°, while for LAE442 it was 49°. The samples with the applied ALD coating show a much higher angle, equal to AE42–270° and LAE442–230°,

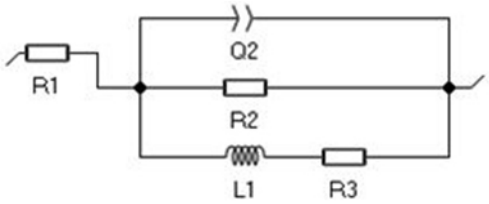

Fig. 6. Equivalent circuit that represents the impedance spectra

respectively. The PVD-coated samples are characterized by the smallest phase shift angles, 45° for AE42 and 35° for LAE442, respectively. The values in Table 2 show the same dependency as in the case of the data from the charts. Figure 6 shows an equivalent circuit that represents the impedance spectra. Table 2 shows the values of the individual system components for each sample.

Figures 7 and 8 show the surface of samples after the corrosion process. In the case of non-corrosive surfaces, distinct pitting is visible. In the case of the sample made of the LAE442

a) b)

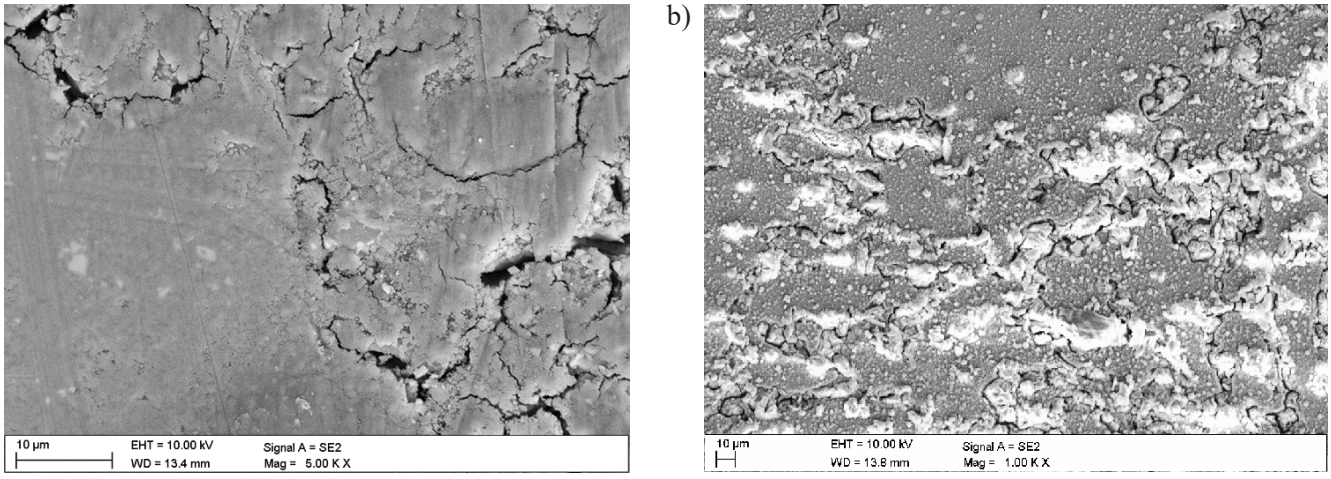

Fig. 7. Surface morphology following electrochemical examination of the uncoated sample: a) AE 42 alloy b) LAE 442 alloy

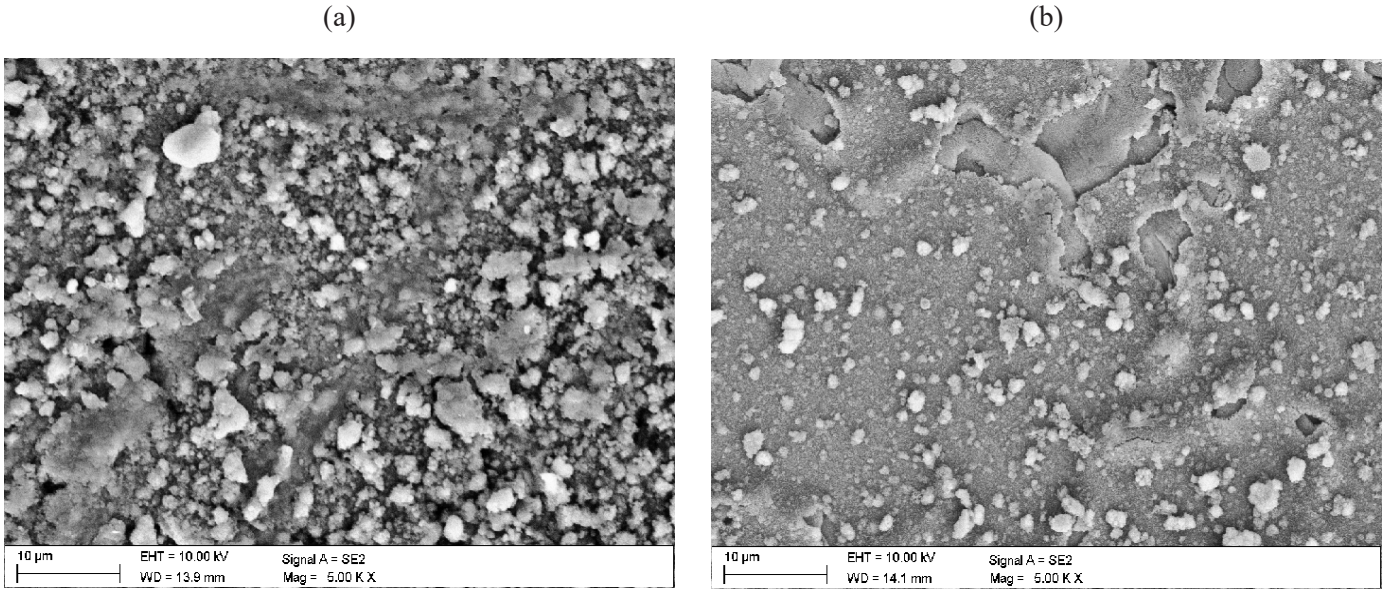

Fig. 8. Surface morphology following electrochemical examination of the sample coated by: a) Ti/TiO_2 coating b) $Ti/TiO_2/Ti/TiO_2$ coating

alloy, corrosion products, i.e. agglomerates of oxides on the surface, are visible. In the case of the surface of corrosion-coated samples, we also see numerous corrosion products. The corrosion is uniform and has occurred to a greater extent than in the case of uncoated samples. Figure 9 shows the EDS result of the surface of a corroded sample covered with the PVD method. Oxygen peaks are visible, which are the result of the corrosive process. Titanium peaks testify to the continued presence of the coating on the surface even after the corrosion process.

Based on tests using the transmission electron microscope, the TiO_2 coating obtained by the ALD method was characterized and the transition zone between the substrate and coating was examined. As a result of the research, two zones of structures were specified, starting from the substrate: sublayer and specific TiO_2 layer (Fig. 10). A large amount of oxygen in the sublayer (area X2, Fig. 10a, EELS spectrum, Fig. 10d) may indicate that the coated surface was oxidized, which is typical for this type of substrate material. EELS spectral analysis also confirms, as assumed, the presence of the elements of titanium and oxygen in the titanium oxide specific layer (Fig. 10d). Moreover, TEM research shows that the TiO_2 layer obtained by the ALD method has a structure similar to an amorphous one, which is also confirmed by the analysis of electron diffraction (Fig. 10c).

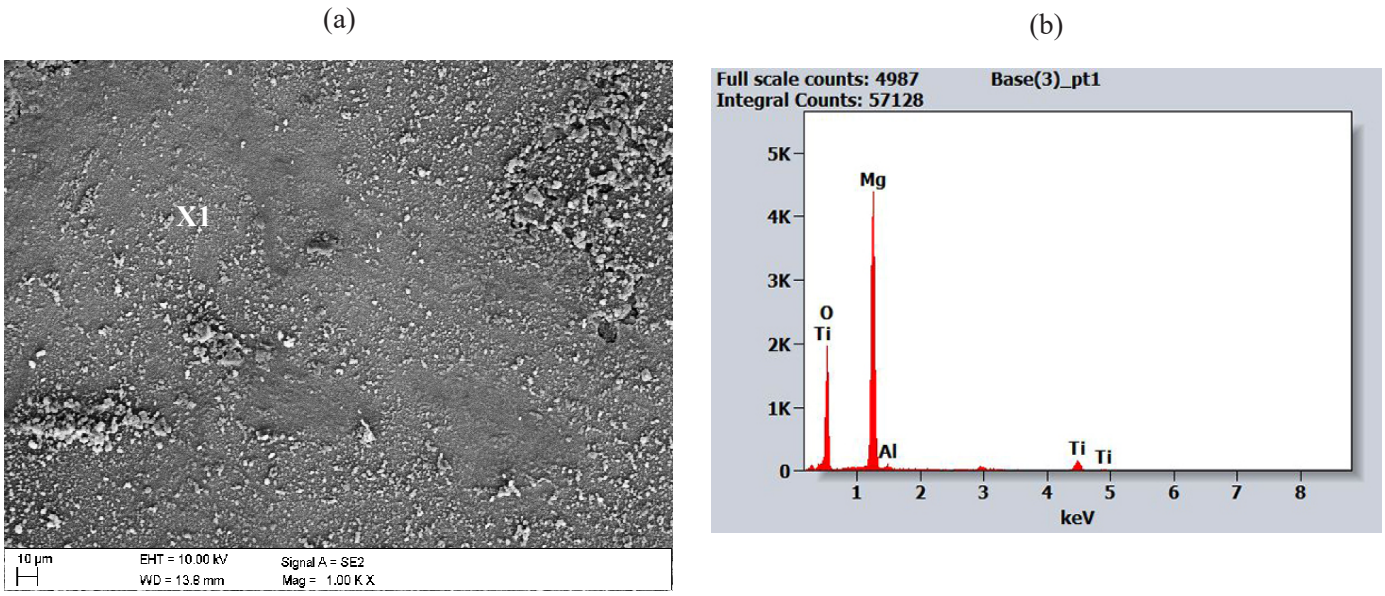

Fig. 9. a) Surface topography of Ti/TiO_2 coating on the AE42 alloy substrate after corrosion process, b) scattered X-ray energy diagram from micro-area X1 according to Fig. 13a, SEM

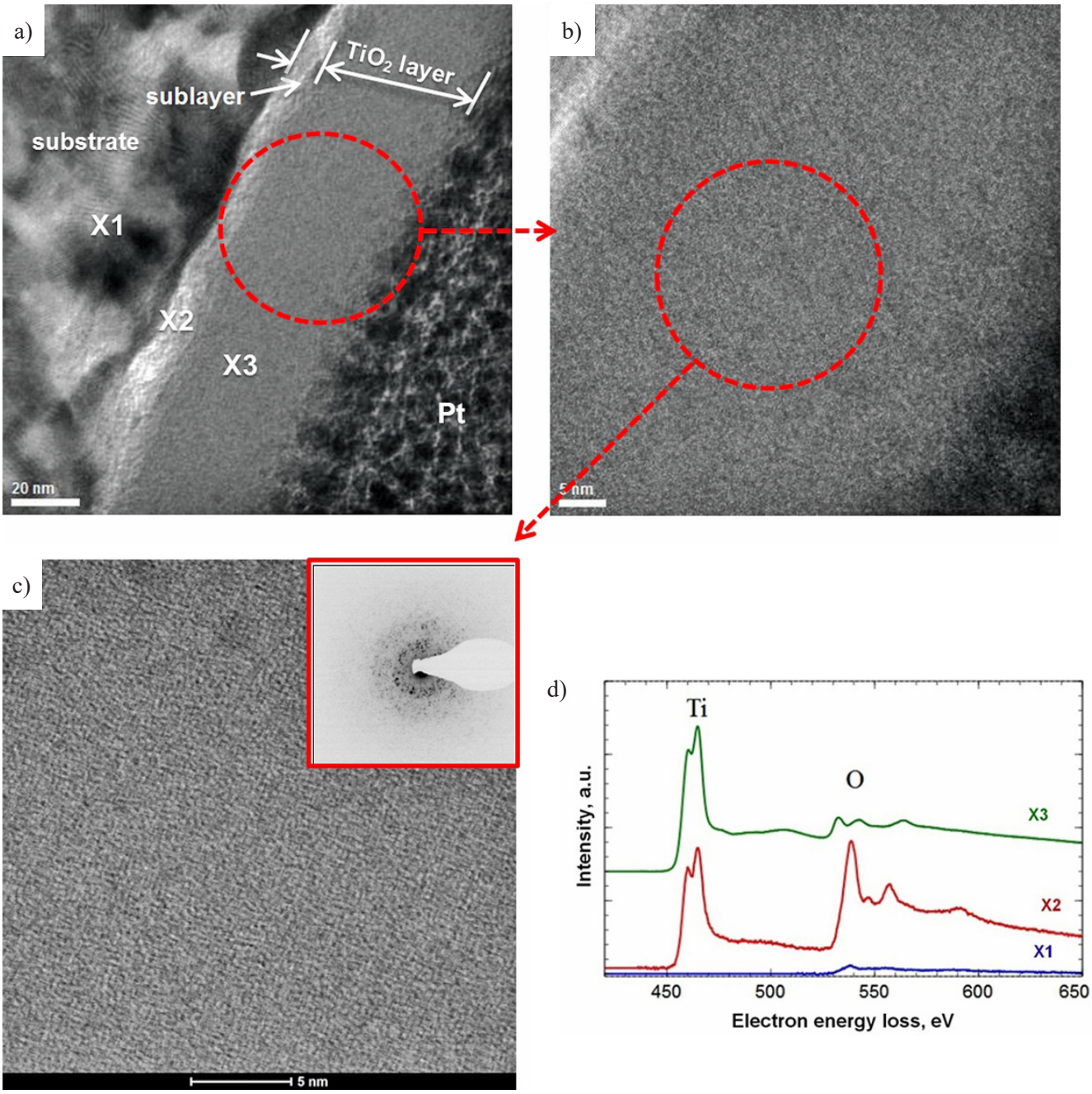

Fig. 10. Structure (TEM) of TiO_2 coating obtained: a–c) bright field (c with diffraction pattern); d) EELS energy loss spectrum from areas X1, X2, and X3 according to figure a

3.3. Wear resistance test

As a result of the ball-on-plate wear resistance test of the uncoated substrate materials, it was found that the friction coefficient for both magnesium alloys is equal and amounts to approximately $\mu = 0.4$. In the case of plots of friction coefficients for samples coated with the tested coatings, an initially low friction coefficient of about $\mu = 0.2$ is observed, which corresponds to the friction of the counter-sample against the coated surface. After a certain number of cycles, a gradually increasing friction coefficient is observed to the value of $\mu = 0.4$, corresponding to the friction of the oxide counter-sample against the magnesium substrate. The number of cycles after which the coating is broken and the friction coefficient increases were assumed as the cycles' critical C_c. Since the increase of the friction coefficient occurs gradually, the number of cycles for which the friction coefficient exceeds the value of $\mu = 0.3$ was assumed as C_c (Fig. 11). Based on the performed tests, it was found that the TiO_2 coating obtained by the ALD method on the substrate of the Mg-4Li-4Al-2RE type, for which C_c is 64 cycles, shows the highest abrasion resistance (Fig. 11 and 12). As a result of the observation of the surface of the tested samples with the use of a scanning electron micro-

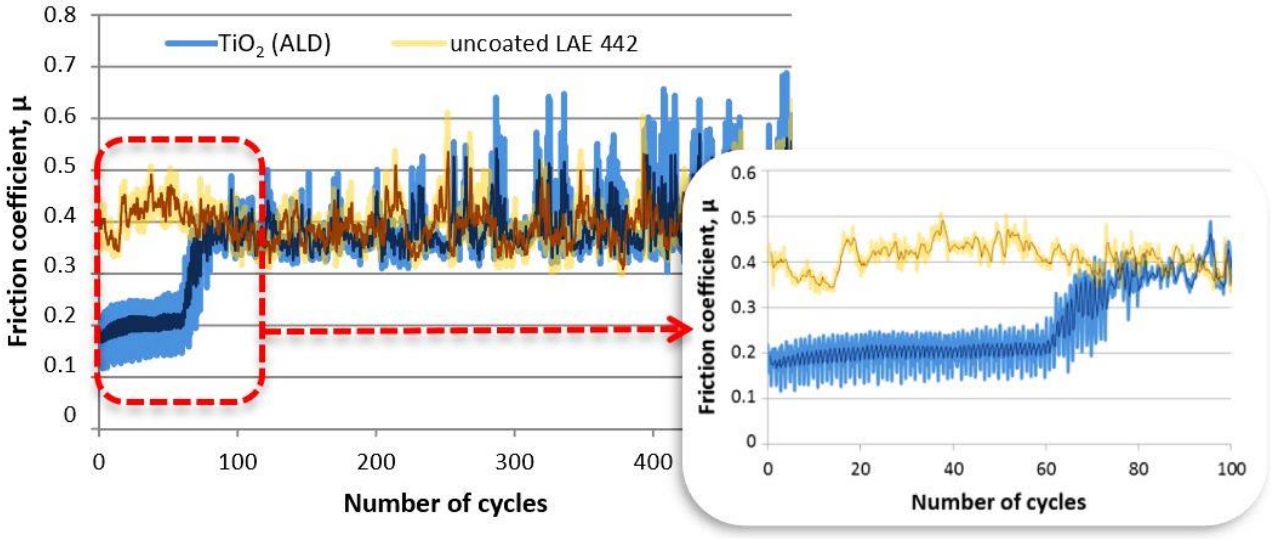

Fig. 11. Friction coefficient as a function of the number of cycles for uncoated Mg-4Li-4Al-2RE substrate material and TiO_2 coating obtained by ALD method

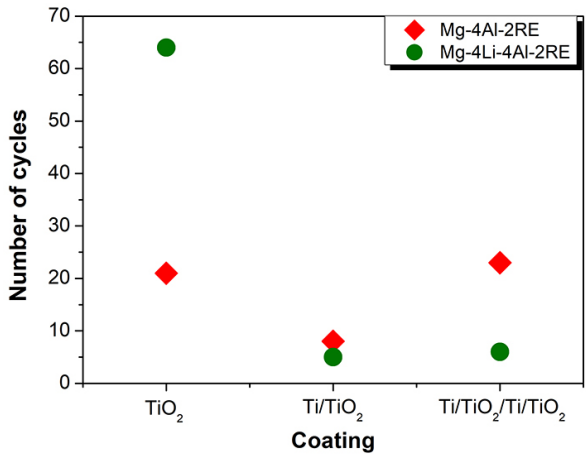

Fig. 12. Comparison of the critical number of cycles C_c of the tested PVD and ALD coatings on Mg-4Al-2RE and Mg-4Li-4Al-2RE magnesium alloy substrates

scope, it was found that the main wear mechanism was abrasion and surface oxidation, as evidenced by the presence of areas rich in magnesium and oxygen (Fig. 13). Also, chipping and cracks in the coating were found near the edge of the abrasion paths (Fig. 13b). SEM and EDS tests of ceramic counter-samples showed the formation of a build-up of magnesium oxide on their surface (Fig. 14).

4. SUMMARY

Magnesium alloys are among the lightest construction materials and are therefore increasingly popular in the industry. They are also characterized by low cost, good mechanical properties and the ability to dampen vibrations. One of the key factors limiting their wider application is their low corrosion resistance, which significantly reduces potential application properties. The TiO_2 coating is often used as corrosion protection due to its physical and chemical stability properties, especially in acidic environments. The magnetron method of depositing the Ti/TiO_2 coating on two magnesium alloys of the Mg-(Li)-Al-RE type allowed for the deposition of a relatively continuous layer without visible flaking and pores as expected based on relevant literature [17, 18]. The obtained coatings do not improve the corrosion resistance of the alloys. The best results of the potentiodynamic method and electrochemical impedance spectroscopy were obtained for samples coated with the use of the ALD method. This method allows for deposition of high-quality barrier layers [10], which gives better properties than in the layers obtained by the magnetron method. The coating obtained by this method significantly improves the electrochemical properties of the coated magnesium alloys. The layer applied by the ALD method also improves the tribological properties of the sample, affecting the reduction of the friction coefficient between the tested surface and the ceramic counter-sample. Distinctly worse electrochemical properties of PVD coatings may be caused by discontinuities in the coating produced, as a result of which the substrate material was not tightly coated. Consequently, the corrosion rate at the leakage point was greater than in the absence of the protective coating. In the case of both the uncoated materials and those with the deposited coating, the samples of the alloy with lithium as an alloy additive, which lowers the corrosion resistance of magnesium alloys, showed lower corrosion resistance. The produced PVD coating also increased the surface roughness, which is crucial when considering corrosion resistance. Future research should be aimed at optimizing the process conditions obtained by the layer or at combining it with coatings made by means of other methods or of other compounds, producing hybrid coatings, in order to eliminate discontinuities and reduce the roughness of the sample surface.

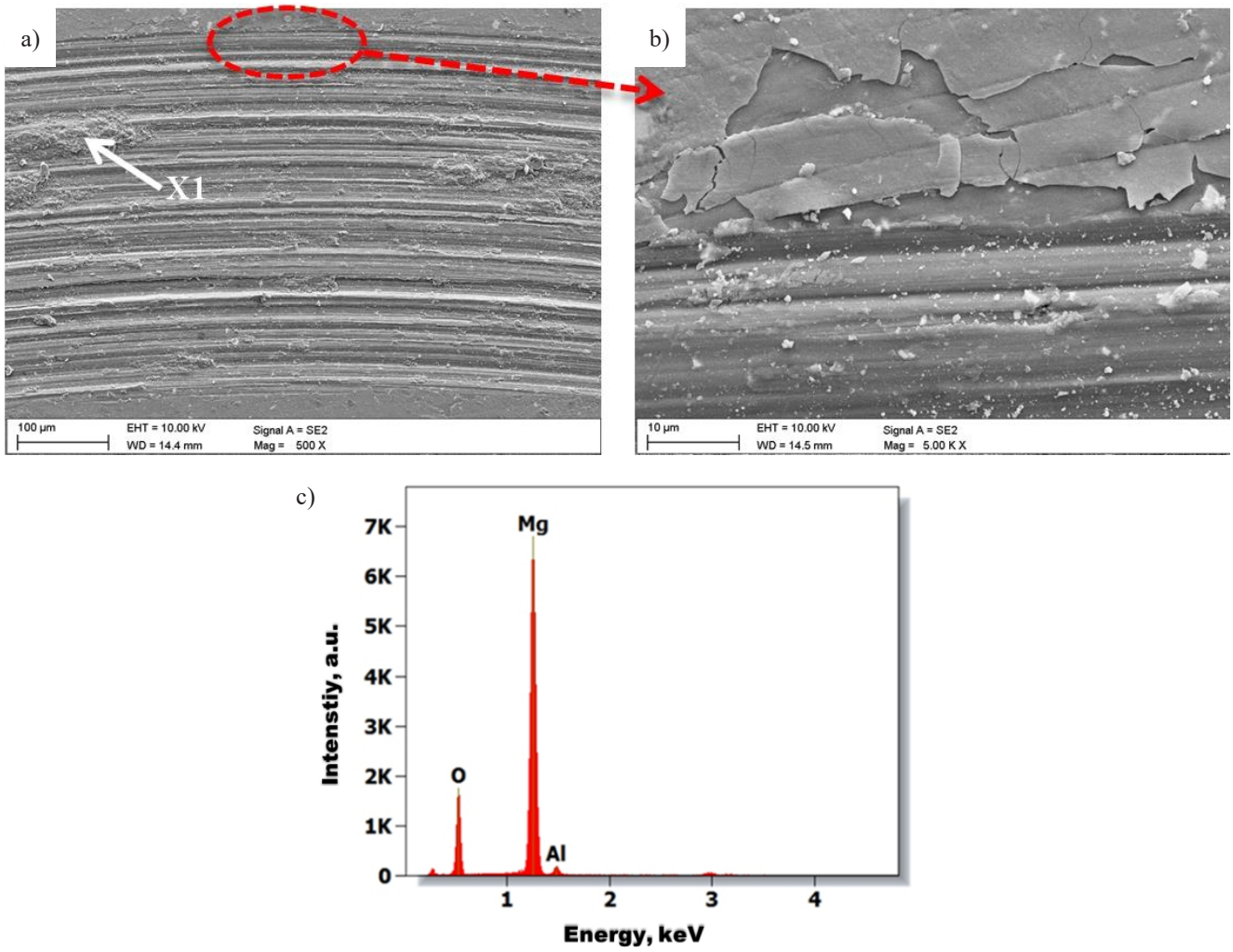

Fig. 13. a, b) Wear trace after the "ball-on-plate" wear test for the TiO_2 layer deposited in ALD process on Mg-4Li-4Al-2RE alloy substrate, c) X-ray energy dispersive plot of the area X1 shown in figure a

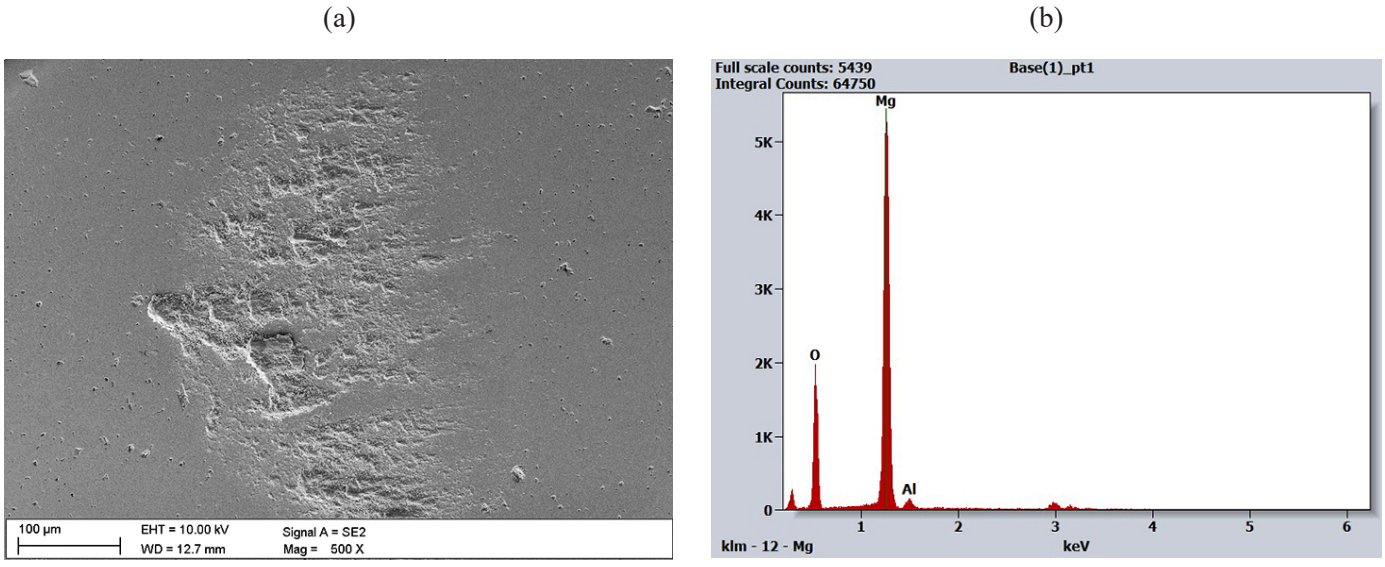

Fig. 14. a) Wear place after the "ball-on-plate" wear test for the Al_2O_3 ball as a counter-sample, b) X-ray energy dispersive plot of the area X1 shown in figure a

ACKNOWLEDGEMENTS

The investigations are co-financed by the International Visegrad Fund through the Visegrad Scholarship Program.

REFERENCES

[1] K.-J. Huang, L. Yan, C.-S. Wang, C.-S. Xie, and C.-R. Zhou, "Wear and corrosion properties of laser cladded $Cu_{47}Ti_{34}Zr_{11}Ni_8$/SiC amorphous composite coatings on AZ91D magnesium alloy", *Trans. Nonferrous Met. Soc. China*, vol. 20, no. 7, pp. 1351–1355, 2010, doi: 10.1016/S1003-6326(09)60303-4.

[2] J. Song, J. She, D. Chen, and F. Pan, "Latest research advances on magnesium and magnesium alloys worldwide", *J. Magnes. Alloy.*, vol. 8, no. 1, pp. 1–41, 2020, doi: 10.1016/j.jma.2020.02.003.

[3] M. Król, P. Snopiński, M. Pagáč, J. Hajnyš, and J. Petrů, "Hot Deformation Treatment of Grain-Modified Mg-Li Alloy", *Materials*, vol. 13, pp. 4557–4570, 2020, doi: 10.3390/ma13204557.

[4] M. Król, "Magnesium–lithium alloys with TiB and Sr additions", *J. Therm. Anal. Calorim.*, vol 138, pp. 4237–4245, 2019, doi: 10.1007/s10973-019-08341-2.

[5] F. Liu, Z. Sun, and Y. Ji, "Corrosion resistance and tribological behavior of particles reinforced AZ31 magnesium matrix composites developed by friction stir processing" *J. Mater. Res. Technol-JMRT*, vol. 11, pp. 1019–1030, 2021, doi: 10.1016/j.jmrt.2021.01.071.

[6] H. Yu, W. Li, Y. Tan, and Y. Tan, "The Effect of Annealing on the Microstructure and Properties of Ultralow-Temperature Rolled Mg–2Y–0.6Nd–0.6Zr Alloy", *Metals*, vol. 11, no 2, pp. 315–331, 2021, doi: 10.3390/met11020315.

[7] K. Cesarz-Andraczke and A. Kazek-Kęsik, "PEO layers on Mg-based metallic glass to control hydrogen evolution rate", *Bull. Pol. Acad. Sci. Tech. Sci.*, vol. 68, no. 1, pp119–124, 2020, doi: 10.24425/bpasts.2020.131841.

[8] L. Zhu and G. Song, "Improved corrosion resistance of AZ91D magnesium alloy by an aluminum-alloyed coating" *Surf. Coat. Technol.*, vol. 200, No. 8, pp. 2834–2840, 2006.

[9] J.D. Majumdar, R. Galun, B.L. Mordike, and I. Manna, "Effect of laser surface melting on corrosion and wear resistance of a commercial magnesium alloy", *Mater. Sci. Eng. A*, vol. 361, no. 1–2, pp. 119–129, 2003.

[10] A. Woźniak, W. Walke, A. Jakóbik-Kolon, B. Ziębowicz, Z. Brytan, and M. Adamiak "The Influence of ZnO Oxide Layer on the Physicochemical Behavior of Ti6Al4V Titanium Alloy" *Materials*, vol. 14, p. 230, 2021, doi: 10.3390/ma14010230.

[11] F. Vargas, H. Ageorges, P. Fournier, P. Fauchais, and M.E. López, "Mechanical and tribological performance of Al_2O_3-TiO_2 coatings elaborated by flame and plasma spraying", *Surf. Coat. Technol.*, vol. 205, pp. 1132–1136, 2010, doi: 10.1016/j.surfcoat.2010.07.061.

[12] H. Hu, X. Nie, and Y. Ma, "Corrosion and Surface Treatment of Magnesium Alloys", in *Magnesium alloys properties in solid and liquid states*, vol. 3, pp. 67–108, 2013, doi: 10.1155/2013/532896.

[13] K.J. Singh, M. Sahni, and M. Rajoriya, "Study of Structural, Optical and Semiconducting Properties of TiO_2 Thin Film deposited by RF Magnetron Sputtering", *Mater. Today: Proc.*, vol. 12, no. 3, pp. 565–572, 2019.

[14] T. Tański, W. Matysiak, D. Kosmalska, and A. Lubos "Influence of calcination temperature on optical and structural properties of TiO_2 thin films prepared by means of sol-gel and spin coating", *Bull. Pol. Acad. Sci. Tech. Sci.*, vol. 66, no. 2, pp. 151–156, 2018, doi: 10.24425/119069.

[15] Y. Zhao, Z. Zhang, L. Shi, F. Zhang, S. Li, and R. Zeng, "Corrosion resistance of a self-healing multilayer film based on SiO_2 and CeO_2 nanoparticles layer-by-layer assembly on Mg alloys", *Mater. Lett.*, vol. 237, pp. 14–18, 2019.

[16] K. Trembecka-Wojciga, R. Major, J.M. Lackner, F. Bruckert, E. Jasek, and B. Major, "Biomechanical properties of the thin PVD coatings defined by red blood cells", *Bull. Pol. Acad. Sci. Tech. Sci.*, vol. 63, no. 3, pp. 697–705, 2015, doi: 10.1515/bpasts-2015-0081.

[17] A. Kania, W. Pilarczyk, and M.M. Szindler, "Structure and corrosion behavior of TiO2 thin films deposited onto Mg-based alloy using magnetron sputtering and sol-gel", *Thin Solid Films*, vol. 701, pp. 252–259, 2020, doi: 10.1016/j.tsf.2020.137945.

[18] P. Pansila, N. Witit-anunb, and S. Chaiyakun, "Influence of sputtering power on structure and photocatalyst properties of DC magnetron sputtered TiO_2 thin film", *Procedia Eng.*, vol. 32, pp. 862–867, 2012.

[19] M. Basiaga, W. Walke, M. Staszuk, W. Kajzer, A. Kajzer, and K. Nowińska, "Influence of ALD process parameters on the physical and chemical properties of the surface of vascular stents", *Arch. Civ. Mech. Eng.*, vol. 17, pp. 32–42, 2017, doi: 10.1016/j.acme.2016.08.001.

[20] L. Velardi, L. Scrimieri, L. Maruccio, V. Nassisi, A. Serra, D Manno, L. Calcagnile, and G. Quarta, "Synthesis and doping of TiO_2 thin films via a new type of laser plasma source", *Vacuum*, vol. 184, p. 109890, 2021, doi: 10.1016/j.vacuum.2020.109890.

[21] A. Kozlovskiy, I. Shlimas, K. Dukenbayevc, and M. Zdorovets, "Structure and corrosion properties of thin TiO_2 films obtained by magnetron sputtering", *Vacuum*, vol. 164, pp. 224–232, 2019, doi: 10.1016/j.vacuum.2019.03.026.

[22] M. Esmaily *et al.*, "Fundamentals and advances in magnesium alloy corrosion", *Prog. Mater. Sci.*, vol. 89, pp. 92–193, 2017, doi: 10.1016/j.pmatsci.2017.04.011.

[23] W. Zhang, W. Liu, B. Li, and G. Mai, "Characterization and Tribological Investigation of Sol-Gel Titania and Doped Titania Thin Films", *J. Am. Ceram. Soc.*, vol. 85, no. 7, pp. 1770–1776, 2002, doi: 10.1111/j.1151-2916.2002.tb00351.x.